Eroding dynamic topography

J. Braun,[1] X. Robert,[1] and T. Simon-Labric[1]

Received 10 January 2013; revised 28 February 2013; accepted 28 February 2013.

[1] Geological observations of mantle flow-driven dynamic topography are numerous, especially in the stratigraphy of sedimentary basins; on the contrary, when it leads to subaerial exposure of rocks, dynamic topography must be substantially eroded to leave a noticeable trace in the geological record. Here, we demonstrate that despite its low amplitude and long wavelength and thus very low slopes, dynamic topography is efficiently eroded by fluvial erosion, providing that drainage is strongly perturbed by the mantle flow driven surface uplift. Using simple scaling arguments, as well as a very efficient surface processes model, we show that dynamic topography erodes in direct proportion to its wavelength. We demonstrate that the recent deep erosion experienced in the Colorado Plateau and in central Patagonia is likely to be related to the passage of a wave of dynamic topography generated by mantle upwelling. **Citation:** Braun, J., X. Robert, and T. Simon-Labric (2013), Eroding dynamic topography, *Geophys. Res. Lett.*, *40*, doi:10.1002/grl.50310.

1. Introduction

[2] Dynamic topography is the surface expression of mantle convection, resulting from the topographic load necessary to balance the viscous stresses originating from mantle flow at the base of the lithosphere [*Hager et al.*, 1985]. Revisiting poorly understood aspects of the geological record combined with sophisticated modeling of mantle flow has recently led to renewed interest in constraining and quantifying the dynamic contribution to surface topography [*Mitrovica et al.*, 1989; *Gurnis et al.*, 2000; *Conrad and Gurnis*, 2003; *Forte et al.*, 2007; *Hartley et al.*, 2011]. A summary of recent investigations on the subject can be found in *Braun* [2010].

[3] Understanding and constraining present and past dynamic topography is critical to evaluate its contribution to global and local sea-level changes [*Moucha et al.*, 2008; *Conrad and Husson*, 2009], decipher unexplained parts of the geological record such as the occurrence of broad continental inundation [*Gurnis*, 1993] or uplift [*Bertelloni and Gurnis*, 1997; *Gurnis et al.*, 2000]. Most interestingly perhaps, studying dynamic topography has revealed rather unexpected links between the dynamics of the Earth's deep interior and its surface components, such as potential perturbation to oceanic circulation [*Poore and White*, 2011], large scale continental drainage reorganizations [*Shephard et al.*, 2010] or the formation of major geomorphic features such as the Grand Canyon [*Karlstrom et al.*, 2008].

[4] Interestingly, quantifying the amplitude and scale (extent) of present-day dynamic topography is rather difficult as it depends on a good knowledge of crustal and lithospheric structures, necessary to compute the isostatically compensated contribution to surface topography, as shown in the variability of past and recent estimates [*Bertelloni and Gurnis*, 1997; *Gurnis et al.*, 2000; *Moucha et al.*, 2007; *Steinberger*, 2007; *Heine et al.*, 2008; *Conrad and Husson*, 2009]. Consequently, the amplitude and timing of dynamic topography might be better constrained by interrogating the past, whether it is through the sedimentary [*Mitrovica et al.*, 1989; *Heine et al.*, 2008], geomorphological [*Hartley et al.*, 2011] or thermochronological record [*Flowers and Schoene*, 2010], as the time-integrated effect of mantle flow is less sensitive to our knowledge of crustal thickness.

[5] However, in part due to its transient nature, and in part to its relatively low amplitude (<1000 m), a direct record of dynamic topography is difficult to obtain the resulting uplift leads to subaerial exposure of rocks, as our tools for constraining paleo-elevations remain rather imprecise [*Rowley*, 2007; *Peppe et al.*, 2010] and our best hope of documenting past dynamic topography requires that it be eroded to produce a sedimentary or geomorphologic record or reset thermochronological system by exhumation-induced rock cooling. Interestingly, the very nature of the dynamic topography (low amplitude, long wavelength and slowly changing) makes it, apparently, unlikely to be affected by erosion [*Braun*, 2010], which requires large slopes and rapid uplift to be efficient.

[6] In this paper, we will show that, contrary to this view, dynamic topography is in many situations a transient feature and, using the most widely accepted parameterization of fluvial erosion, we will demonstrate that it is likely to be efficiently eroded away by surface processes and, consequently, permanently recorded in a measurable way in the geological record. To achieve this, we will use a recently developed surface processes model (FastScape; *Braun and Willett* [2013]) that is highly efficient and can thus be used to study the erosion of very large scale ($\approx$ 1000 km) surface topography at a resolution (<1000 m) that is sufficient to capture local slopes and drainage evolution.

2. Fluvial Erosion and Dynamic Topography

[7] Although mantle flow is relatively steady over tens to hundreds of millions of years, and the dynamic topography that it creates should therefore remain unchanged over the same periods of time, the relative motion of tectonic plates

All Supporting Information may be found in the online version of this article.

[1]ISTerre Université de Grenoble 1, CNRS-IRD, F-38041 Grenoble, France.

Corresponding author: J. Braun, ISTerre Université de Grenoble 1, CNRS, F-38041 Grenoble, France. (Jean.Braun@ujf-grenoble.fr)

0094-8276/13/10.1002/grl.50310

Table 1. Numerical Model Parameter Values[a]

Parameter	Value
K_f	4.7×10^{-6} to 10^{-7} $m^{0.2}$/yr
m	0.4
n	1
K_D	0, 0.01, 0.1, 1 m^2/yr
E	10^{11} Pa
T_e	20 km
ν	0.25
ρ_c	2800 kg/m^3
ρ_a	3200 kg/m^3

[a]All experiments are 50 Myr in duration, with an initial 10 Myr phase of uplift and establishment of the dynamic topography followed by a 40 Myr period of migration of the plate at a rate of 25 km/Myr.

with respect to the underlying mantle can cause dynamic topography—as experienced by an observer attached to the moving surface plates—to be transient [*Gurnis et al.*, 1998], as shown in numerous recent studies of reconstructed past dynamic topography [*Moucha et al.*, 2009]. To illustrate this point, let us parameterize, to first order, the dynamic topography caused by a mantle plume or upwelling of width 2λ beneath a plate that moves at a velocity v in the x-direction by the following Gaussian function:

$$z(x) = z_0 e^{-(x-vt)^2/\lambda^2} \tag{1}$$

where z_0 is the maximum amplitude of the dynamic topography, and t, is time. The resulting rate of uplift/subsidence is given by

$$\dot{z}(x) = v\frac{\partial z}{\partial x} = -\frac{2vz_0(x-vt)}{\lambda^2}\, e^{-(x-vt)^2/\lambda^2} \tag{2}$$

which implies that the surface is uplifted in front of the plume and subsides behind it at a rate that is proportional to the plate velocity ($\approx$ 10 cm/yr) and modulated by the slope of the topography ($\approx 10^{-3}$).

[8] Because it is driven by mantle flow, dynamic topography must remain relatively unchanged (to balance the viscous stress applied at the base of the lithosphere) even if it is eroded away. The characteristic time for adjustment

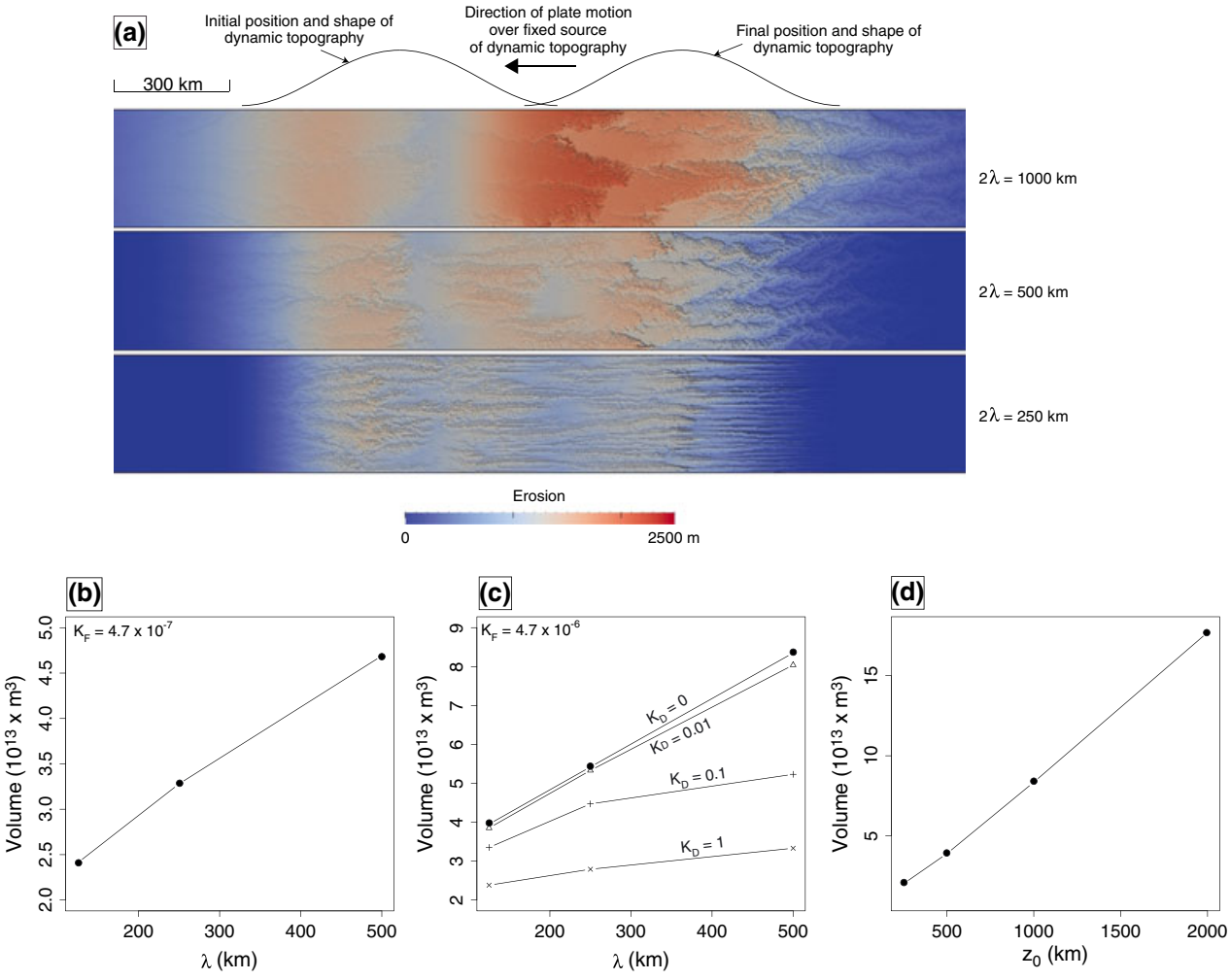

Figure 1. (a) Time integrated erosion computed from the landscape evolution model using different dynamic topography wavelength (2λ), showing the direct, quasi-linear dependency on wavelength, as suggested by equation 4. Here, $K_f = 4.7 \times 10^{-6}$. The two curves on top of Figure 1a show the initial and final position and shape of the imposed vertical stress at the base of the plate for the case (λ = 250 km); Total volume eroded over the passage of the "wave" of dynamic topography (b) as a function of imposed wavelength and (c) various values of the diffusion coefficient, K_D, and (d) as a function of dynamic topography amplitude (no diffusion).

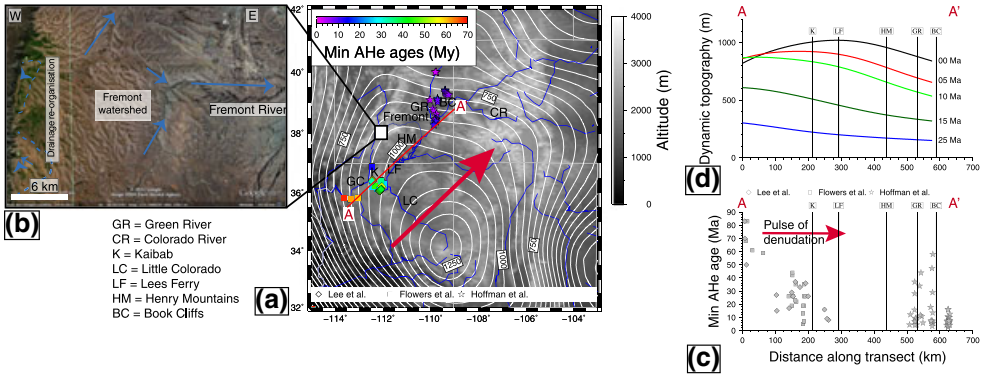

Figure 2. Geomorphic evolution of the Colorado Plateau and dynamic topography. (a) Shaded DEM of the Colorado Plateau; white contour curves draw the present-day dynamic topography with 50 m intervals [*Moucha et al.*, 2009]; the red arrow represent the movement of the dynamic topography swell in the last 30 My; diamonds, squares and stars represent minimum apatite (U-Th)/He ages, respectively, from *Lee*, [2008]; *Lee et al.*, [2011], *Flowers et al.*, [2008] and *Hoffman*, [2009]; *Hoffman et al.*, [2011]; the red line AA is the transect used to build Figures 2c and 2d; Blue curves represent the drainage network; grey lines mark states boundaries. (b) Zoom of the area included in the white square from the Figure 2a showing the drainage inversion from west to east happening in the upper part of the Fremont River; blue arrows show present day drainage direction, dashed line marks zone with drainage reorganization. (c) Projection of the minimum apatite (U-Th)/He ages along the transect AA showing a decrease of the ages following the displacement of the wave of dynamic topography. (d) Evolution of the dynamic topography since 25 Ma along the transect AA extracted from the global model Tx07v2 from *Moucha et al.*, [2009].

of dynamic topography to surface erosion is set by asthenospheric viscosity, and is thus similar to glacial rebound time ($1 - 5 \times 10^4$ years). This means that, on geological time scales, a kilometer of dynamic topography could lead to several kilometers of erosion. The limit is set by the deflection of the crust-mantle boundary that would create a gravitational stress equivalent to the viscous mantle stress, given by $z_{\text{Moho}} \approx z_0\rho_c/(\rho_m - \rho_c) \approx 7z_0$, where z_0 is surface deflection (and erosion) and ρ_c and ρ_m are crustal and mantle densities, respectively.

[9] With this in mind, let us now consider how much a river network can erode from the surface of a continent that is subjected to a "wave" of dynamic topography. For this, we will apply the basic stream power law [*Howard and Kerby*, 1983] that states that fluvial erosion, $\dot{e}$, is proportional to drainage area, A, and local slope S: $\dot{e} = K_f S^n A^m$ to the topographic profile depicted by equation (1). The parameters n and m are not well constrained but their ratio is better known ($n/m \approx 2$) as it controls the steady-state profile or "concavity" of river channels [*Whipple and Tucker*, 1999]. The value of K_f depends on climate and lithology and is quite variable. Drainage area is known to vary as a distance to topographic divide, d, according to: $A = kd^h$ [*Hack*, 1960] where k and h are constant and $h \approx 2$. Assuming that erosion does not affect dynamic topography and that the divide therefore remains located on top of the "passing" plume, we can write the following:

$$\dot{e} = K\left|-\frac{2z_0}{\lambda}\frac{x-vt}{\lambda}e^{-\left(\frac{x-vt}{\lambda}\right)^2}\right|^n |x-vt|^{mh} = \frac{2Kz_0^n}{\lambda^{2n}}|x-vt|^{n+mh}e^{-\left(\frac{x-vt}{\lambda}\right)^2} \quad (3)$$

where $K = K_f k^n$. Integrating this expression over time, we obtain the total, maximum erosion, e, that the continental surface experiences, which after some algebra (see Supporting Information A) gives:

$$e = \int_{-\infty}^{+\infty} \dot{e}_{(x=0)}\, \mathrm{d}t \propto \frac{z_0^n \lambda^{1+mh-n}}{v} = \frac{z_0^n \lambda}{v} \quad (4)$$

as $1 + mh - n \approx 1$, demonstrating that erosion of dynamic topography increases linearly with its wavelength. This is a consequence of the strong dependence of drainage area on λ, which dominates over its control on slope.

3. Numerical Modeling

[10] This result depends on several assumptions, namely that the dynamic topography controls the geometry of the drainage system and that the slope that sets the erosional efficiency is the regional slope. Both assumptions need to be tested. To do this, we have used a recently developed and highly efficient algorithm [*Braun and Willett*, 2013] to solve the stream-power law on an evolving plan-form topographic corridor of dimension 3000×300 km, moving on top of a region of mantle upwelling represented by a Gaussian shaped vertical stress applied at the base of a thin elastic plate linked to the surface evolution model. We have computed the resulting evolving topography and time-integrated erosion for three values of the half-wavelength of the topography, λ =125, 250 and 500 km. The value of the other model parameters are given in Table 1 and the Supporting Information B as well as a description of the basic ingredients of the model. The results are shown in Figure 1a as maps of total erosion showing an increase in maximum and mean total erosion with increasing wavelength (λ) as well as plots of total eroded volume as a function of topographic wavelength (Figures 1b and 1c). They also show a weaker

dependency of erosion on dynamic topography amplitude, z_0, as suggested by equation (4). The 1D geometry used in these models has been chosen to verify the analytical solution (equation 4); numerical model runs performed using a more realistic circular geometry for the Gaussian-shaped vertical stress lead to a stronger dependency on λ as $e \propto \lambda^{1.3}$.

[11] This result clearly demonstrates that dynamic topography, despite the small slopes that it engenders, is very amenable to surface erosion by fluvial processes, because fluvial erosion rate depends on drainage area and dynamic topography is capable of controlling drainage network geometry to cause an amplification of discharge. In the model experiments shown in Figure 1a, the main drainage divide position is completely controlled by the dynamic topography, as the initial topography is assumed to be flat, but, under natural conditions, the existence of a strongly entrenched drainage network predating the phase of dynamic topography, i.e., resulting from a previous phase of uplift and erosion, may override this control and prevent the reorganization of drainage. Thus, the mechanism proposed here to efficiently erode long-wavelength dynamic topography is not universal and episodes of uplift (or subsidence) associated with mantle flow may, in some cases, be difficult to decipher from the geological record.

4. Evidence from the Geological Record

[12] In the following section, we present two examples of documented surface uplift associated with a wave of dynamic topography that strongly perturbed surface drainage patterns, which, following our model, explain why they resulted in substantial erosion over a broad area as documented by low temperature thermochronometry.

[13] *Moucha et al.* [2009] and *Robert et al.* [2011] propose, from backwards in time global convection modeling, the passing of a wave of dynamic topography through the Colorado Plateau to explain the 1400 m present-day mean altitude. The consequences of the wave propagation are best described in three phases: (i) global plateau uplift between 30 and 15 Ma; (ii) tilting of the plateau to the east between 15 and 5 Ma, and (iii) a back tilt of the western part of the plateau to the west since 5 Ma [*Robert et al.*, 2011]. The Colorado River controls the main drainage of the Colorado Plateau; it is currently flowing from the northeast to the southwest, following the dynamic uplift wave propagation direction, and thus probably controlled by the mantle time-evolution. Even if the course of the Colorado River and its drainage system are not well constrained before 5 Ma, some elements argue for a strong drainage perturbation and reorganization in the last 30 Ma, perturbations that can be explained by the passing of a wave of dynamic uplift. These pieces of evidence include the following: (1) Before 30 Ma, the general flow was to the north [*Holm*, 2001]; (2) The presence of lake paleo-sediments in the plateau interior dated from 16 to 5 Ma [*Spencer et al.*, 2008]; (3) There is no evidence of Colorado Plateau sediments in the Gulf of California prior to 5.3 Ma [*Dorsey et al.*, 2007]; (4) Sudden increase in water flow, associated with the integration of the Lower Colorado River by lake fill and potential spill [*House et al.*, 2008]; (5) Locally, there are perturbed drainage networks with the presence

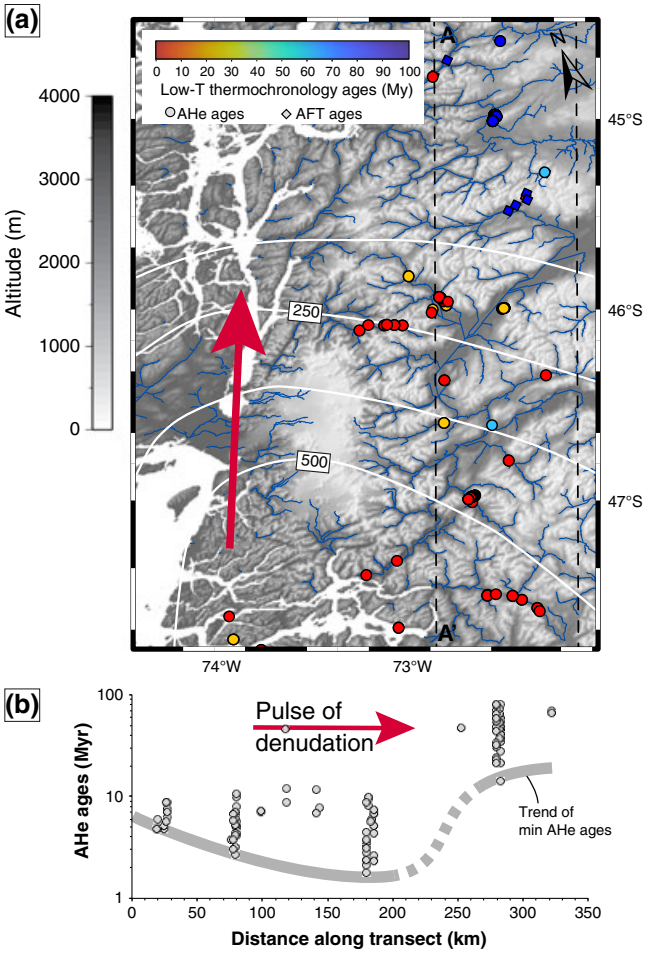

Figure 3. Geomorphic evolution of the Central Patagonia and dynamic topography. (a) Shaded DEM of central Patagonia; white contours show predicted present-day dynamic topography with 125 m intervals; red arrow represents the movement of the dynamic topography swell for the last 10 My; Diamonds and circles represent apatite Fission Tracks and (U-Th)/He ages from [*Thomson et al.*, 2010; *Haschke et al.*, 2006; *Guillaume et al.*, 2013]; blue lines represent drainage network. (b) Projection of the apatite (U-Th)/He ages along the transect AA showing a decrease of minimum ages following the northward displacement of the wave of dynamic topography and a major increase of ages north of the present-day location of the wave of dynamic topography. The gray line highlights the trend of minimum ages.

of reused paleo-drainage, indicating inverse flow directions [see Figures 2a and 2b]. Low-temperature thermochronological data (such as (U-Th)/He on apatite) provides constraints on the timing of about 1 to 2 km of denudation from the top of the Plateau [*Flowers et al.*, 2008; *Lee*, 2008; *Lee et al.*, 2011; *Hoffman*, 2009; *Hoffman et al.*, 2011] and suggests an increase in total erosion from the southwest to the central Plateau [see Figure 2c], which may correspond to a wave of erosion induced by the propagation of a pulse of dynamic topography (Figures 2c and 2d). It demonstrates that dynamic topography may lead to signifi-

cant erosion, of amplitude equal or larger to the amplitude of the topography, in association with a main reorganization of drainage patterns.

[14] The Chile Triple Junction episodically migrated northward during the past 14 Ma from 54°S to its present-day position at 46°30S, as several, almost trench-parallel spreading segments entered the subduction. This migration resulted in the opening of an asthenospheric window below Patagonia, inducing a disturbance in the regional mantle flow and the northward migration of a wave of dynamic topography uplifting the overriding plate [*Breitsprecher and Thorkelson*, 2009; *Scalabrino et al.*, 2009; *Guillaume et al.*, 2009]. The northward displacement of this wave of dynamic topography is clearly correlated to (i) a younging in bedrock low-temperature cooling ages towards higher latitudes (46°S to 48°S) corresponding to a wave of late Cenozoic erosion along the eastern flank of the Central Patagonian Andes (Figure 3; [*Guillaume et al.*, 2013]); (ii) the increased height of the orogenic divide at these latitudes (Figure 3; [*Thomson et al.*, 2010]); (iii) the modification of the drainage network in the eastern foreland since at least the late Miocene [*Guillaume et al.*, 2009]. All of these observations support substantial erosion of the dynamic topography enhanced by the reorganization of the drainage system, despite the relatively high preexisting relief and entrenchment of preexisting valleys.

5. Discussion

[15] The total amount eroded from the landscape following the passage of a wave of dynamic topography is linearly dependent on the assumed value for the erosional parameter (or constant) K_f. This parameter is relatively poorly constrained, but some quantitative estimates exist such as those obtained by directly dating magmatic intrusion along the East coast of Australia and measuring how they are affected by erosion [*van der Beek and Bishop*, 2003], or the propagation of knickpoints to form hanging valleys in the French Alps [*Valla et al.*, 2010]. For values of $n = 1$ and $m = 0.4$ as assumed in this study, K_f varies between 5×10^{-7} and 1×10^{-5} $m^{-0.2}$ y^{-1}. Using a similar range of values, we predict from a range of model runs that, locally, erosion of a 1000 km wide and 1000 m high wave of dynamic topography can reach several thousands of meters (see results Figure 1), well enough to reset low-temperature thermochronological systems such as He in apatite or even fission track in apatite. The volumes of sediments that are generated are also very large, between 10^{13} and 10^{14} m^3 (see results Figure 1), such that the resulting sedimentary deposits should be easily identified in the geological record.

[16] We demonstrated here that large scale, low amplitude topography can easily be eroded away if one considers the opposing contributions from slope and drainage area in the expression of the stream power law for fluvial erosion. Previous work on the subject often considered that large-scale continental erosion is a transport-limited process that is better represented by a diffusion equation [*Moretti and Turcotte*, 1985]. Under this hypothesis, total integrated erosion following the passage of a wave of dynamic topography scales as the inverse of the wavelength of the topography (see Supporting Information C) and one is led to conclude that dynamic topography is unlikely to be affected by erosion. However, such an approach is difficult to justify theoretically as diffusive transport takes place at the scale of a hillslope and not that of a continent. Adding a diffusion term to the basic erosion law,

$$\dot{e} = K_f S^n A^m + K_D \frac{\partial^2 z}{\partial x^2} \tag{5}$$

with values for K_D, the diffusivity, derived from hillslope measurements [*Martin*, 2000], i.e., in the range 0.01 to 1 m^2 yr^{-1}, leads to a substantial reduction in total eroded volume but does not affect the scaling of erosion with wavelength of dynamic topography (see Figure 1c), unless very large and unreasonable values of the diffusivity are assumed (> 1 m^2 yr^{-1}).

[17] **Acknowledgments.** The work described in this paper was supported by the Canadian Institute for Advanced Research (CIFAR). The authors thank M. Gurnis and an anonymous reviewer for their constructive comments on an earlier version of this manuscript.

References

Bertelloni, C., and M. Gurnis (1997), Cenozoic subsidence and uplift of continents from time-varying dynamic topography, *Geology*, *25*(8), 735.

Braun, J. (2010), The many surface expressions of mantle dynamics, *Nature Geosc.*, *3*, 825–833, doi:10.1038/ngeo1020.

Braun, J., and S. Willett (2013), A very efficient *O*(*n*), implicit and parallel method to solve the basic stream power law equation governing fluvial incision and landscape evolution, *Geomorphology*, *180-181*, 170–179, http://dx.doi.org/10.1016/j.geomorph.2012.10.008.

Breitsprecher, K., and D. Thorkelson (2009), Neogene kinematic history of NazcaAntarcticPhoenix slab windows beneath Patagonia and the Antarctic Peninsula, *Tectonophysics*, *464*, 10–20, doi:10.1016/j.tecto.2008.02.013.

Conrad, C., and M. Gurnis (2003), Seismic tomography, surface uplift, and the breakup of Gondwanaland: Integrating mantle convection backwards in time, *Geochem. Geophys. Geosyst.*, *4*, 1031, doi:10.1029/2001GC000299.

Conrad, C. P., and L. Husson (2009), Influence of dynamic topography on sea level and its rate of change, *Lithosphere*, *1* (2), 110–120, doi:10.1130/L32.1.

Dorsey, R. J., A. Fluette, K. McDougall, B. A. Housen, S. U. Janecke, G. J. Axen, and C. R. Shirvell (2007), Chronology of miocene-pliocene deposits at Split Mountain Gorge, Southern California: A record of regional tectonics and Colorado River evolution, *Geology*, *35*(1), 57–60, doi:10.1130/G23139A.1.

Flowers, R., and B. Schoene (2010), (U-Th)/He thermochronometry constraints on unroofing of the eastern Kaapvaal craton and significance for uplift of the southern African Plateau, *Geology*, *38*, 827–830, doi:10.1130/G30980.1.

Flowers, R., B. Wernicke, and K. Farley (2008), Unroofing, incision, and uplift history of the southwestern Colorado Plateau from (U-Th)/He thermochronometry, *Geol. Soc. Am. Bull.*, *120*, 571–587, doi:10.1130/B26231.1.

Forte, A. M., J. X. Mitrovica, R. Moucha, N. A. Simmons, and S. P. Grand (2007), Descent of the ancient Farallon slab drives localized mantle flow below the New Madrid seismic zone, *Geophys. Res. Lett.*, *34*(4), L04308, doi:10.1029/2006GL027895.

Guillaume, B., C. Gautheron, T. Simon-Labric, J. Martinod, M. Roddaz, and E. Douville (2013), Dynamic topography control on Patagonian relief evolution as inferred from low temperature thermochronology, *Earth Planet. Sc. Lett.*, *364*, 157–167, doi:10.1016/j.epsl.2012.12.036.

Guillaume, B., J. Martinod, L. Husson, M. Roddaz, and R. Riquelme (2009), Neogene uplift of central eastern Patagonia: Dynamic response to active spreading ridge subduction? *Tectonics*, *28*, TC2009, doi:10.1029/2008TC002324.

Gurnis, M. (1993), Phanerozoic marine inundation of continents driven by dynamic topography above subducting slabs, *Nature*, *364* (6438), 589–593.

Gurnis, M., J. Mitrovica, J. Ritsema, and H.-J. van Heijst (2000), Constraining mantle density structure using geological evidence of surface uplift rates: The case of the African Superplume, *Geochem. Geophys. Geosyst.*, *1*, doi:10.1029/1999GC000035.

Gurnis, M., R. Muller, and L. Moresi (1998), Cretaceous vertical motion of Australia and the Australian-Antarctic discordance, *Science*, *279*(5356), 1499–1504.

Hack, T. (1960), Interpretation of erosional topography in humid temperate regions, *Am. J. Sci.*, *258A*, 80–97.

Hager, B., R. Clayton, M. Richards, and R. Comer (1985), Lower mantle heterogeneity, dynamic topography and the geoid, *Nature*, *313*, 541–545.

Hartley, R. A., G. G. Roberts, N. White, and C. Richardson (2011), Transient convective uplift of an ancient buried landscape, *Nature Geosc.*, *4*(8), 562–565, doi:10.1038/ngeo1191.

Haschke, M., E. Sobel, P. Blisniuk, M. Strecker, and F. Warkus (2006), Continental response to active ridge subduction, *Geophys. Res. Lett.*, *33*, L15315, doi:10.1029/2006GL025972.

Heine, C., R. Dietmar Müller, B. Steinberger, and T. Torsvik (2008), Subsidence in intracontinental basins due to dynamic topography, *Phys. Earth Planet. Inter.*, *171* (1-4), 252–264., doi: 10.1016/j.pepi.2008.05.008.

Hoffman, M., D. Stockli, S. Kelley, J. Pederson, and J. Lee (2011), *CREvolution 2 - Origin and evolution of the Colorado River System, workshop abstracts*, in *volume 1210, chapter Mio-Pliocene erosional exhumation of the Central Colorado Plateau, Eastern Utah - New insights from Apatite (U-Th)/He thermochronometry*, U.S. Geological Survey open-file Report, Reston, Virginia, 132–136.

Hoffman, M. D. (2009), Mio-pliocene erosional exhumation of the central Colorado Plateau, eastern Utah: New insights from apatite (U-Th)/He thermochronometry, Master's thesis, University of Kansas.

Holm, R. F. (2001), Cenozoic paleogeography of the central Mogollon Rim-southern Colorado Plateau region, Arizona, revealed by Tertiary gravel deposits, oligocene to pleistocene lava flows, and incised streams, *Geol. Soc. Am. Bull.*, *113*(11), 1467–1485.

House, P. K., P. A. Pearthree, and M. E. Perkins (2008), Stratigraphic evidence for the role of lake spillover in the inception of the lower Colorado River in southern Nevada and western Arizona, *Geol. Soc. Am. Spec. Pap.*, *439*, 335–353, doi:10.1130/2008.2439(15).

Howard, A., and G. Kerby (1983), Channel changes in badlands, *Geol. Soc. Am. Bull.*, *94*, 73952.

Karlstrom, K. E., R. Crow, L. J. Crossey, D. Coblentz, and J. W. Van Wijk (2008), Model for tectonically driven incision of the younger than 6 Ma Grand Canyon, *Geology*, *36*(11), 835–838, doi:10.1130/G25032A.1.

Lee, J., D. Stockli, S. Kelley, and J. Pederson (2011), *CREvolution 2 - Origin and evolution of the Colorado River system, workshop abstracts*, in *Volume 1210, Chapter Unroofing and Incision of the Grand Canyon Region as Constrained Through Low-Temperature Thermochronology*, U.S. Geological Survey open-file Report, Reston, Virginia, 175–179.

Lee, J. P. (2008), Cenozoic landscape evolution of the Grand Canyon Region, Arizona, Master's thesis, University of Kansas.

Martin, Y. (2000), Modelling hillslope evolution: Linear and nonlinear transport relations, *Geomorphology*, *34*, 1–21.

Mitrovica, J., C. Beaumont, and G. Jarvis (1989), Tilting of continental interiors by the dynamical effects of subduction, *Tectonics*, *8* (5), 1079–1094.

Moretti, I., and D. Turcotte (1985), A model for erosion, sedimentation, and flexure with application to New Caledonia, *J. Geol.*, *3*, 155–168.

Moucha, R., A. Forte, J. Mitrovica, D. Rowley, S. Quéré, N. Simmons, and S. Grand (2008), Dynamic topography and long-term sea-level variations: There is no such thing as a stable continental platform, *Earth Planet. Sc. Lett.*, *271*(1-4), 101–108, doi:10.1016/j.epsl.2008.03.056.

Moucha, R., A. M. Forte, J. X. Mitrovica, and A. Daradich (2007), Lateral variations in mantle rheology: Implications for convection related surface observables and inferred viscosity models, *Geophys. J. Int.*, *169*(1), 113–135, doi:10.1111/j.1365-246X.2006.03225.X.

Moucha, R., A. M. Forte, D. B. Rowley, J. X. Mitrovica, N. A. Simmons, and S. P. Grand (2009), Deep mantle forces and the uplift of the Colorado Plateau, *Geophys. Res. Lett.*, *36* (19), L19310, doi: 10.1029/2009GL039778.

Peppe, D. J., D. L. Royer, P. Wilf, and E. A. Kowalski (2010), Quantification of large uncertainties in fossil leaf paleoaltimetry, *Tectonics*, *29*(3), TC3015, doi:10.1029/2009TC002549.

Poore, H., and N. White (2011), Ocean circulation and mantle melting controlled by radial flow of hot pulses in the Iceland plume, *Nature Geosc.*, *4*, 558–561, doi:10.1038/NGEO1161.

Robert, X., R. Moucha, K. X. Whipple, A. M. Forte, and P. W. Reiners (2011), *CREvolution 2 - Origin and evolution of the Colorado River system, workshop abstracts*, in *Volume 1210, Chapter Cenozoic Evolution of the Grand Canyon and the Colorado Plateau Driven by Mantle Dynamics?*, U.S. Geological Survey open-file Report, Reston, Virginia, 238–244. usgs edition.

Rowley, D. B. (2007), *Stable isotope-based paleoaltimetry: Theory and validation*, in *Paleoaltimetry: Geochemical and Thermodynamic Approaches*, edited by Kohn, M., Reviews in Mineralogy and Geochemistry, Chantilly, Virginia, vol. 66, 2352.

Scalabrino, B., Y. Lagabrielle, A. De la Rupelle, J. Malavieille, M. Polv, R. Espinoza, D. Morata, and M. Surez (2009), *Subduction of an active spreading ridge beneath Southern South America: A review of the Cenozoic geological records from the Andean foreland, Central Patagonia (46-47°S)*, in *Subduction Zone Geodynamics*, edited by Lallemand, S., and R. Funiciello, Springer-Verlag, Berlin Heidelberg, 227–246.

Shephard, G., R. Müller, and L. Liu (2010), Miocene drainage reversal of the Amazon River driven by plate-mantle interaction, *Nature Geosc.*, *3*, doi:10.1038/ngeo1017.

Spencer, J. E., G. R. Smith, and T. E. Dowling (2008), Middle to late Cenozoic geology, hydrography, and fish evolution in the American Southwest, *Geol. Soc. Am. Spec. Pap.*, *439*, 279–299.

Steinberger, B. (2007), Effects of latent heat release at phase boundaries on flow in the Earth's mantle, phase boundary topography and dynamic topography at the Earth's surface, *Phys. Earth Planet. Inter.*, *164*(1-2), 2–20, doi:10.1016/j.pepi.2007.04.021.

Thomson, S., M. Brandon, J. Tomkin, P. W. Reiners, C. Vsquez, and N. Wilson (2010), Glaciation as a destructive and constructive control on mountain building, *Nature*, *467*, 313–317, doi:10.1038/nature09365.

Valla, P., P. Van Der Beek, and D. Lague (2010), Fluvial incision into bedrock: Insights from morphometric analysis and numerical modeling of gorges incising glacial hanging valleys (Western Alps, France), *J. Geophys. Res.*, *115*(F2), F02010, doi:10.1029/2008JF001079.

van der Beek, P., and P. Bishop (2003), Cenozoic river profile development in the Upper Lachlan catchment (SE Australia) as a test of quantitative fluvial incision models, *J. Geophys. Res.*, *1108*, 2309, doi: 10.1029/2002JB002125.

Whipple, K., and G. Tucker (1999), Dynamics of the stream-power incision model: Implications for height limits of mountain ranges, landscape response timescales and research needs, *J. Geophys. Res.*, *104*, 17,661–17,674.